

Analytically Tractable Bayesian Deep Q-Learning

LUONG HA NGUYEN* and JAMES-A. GOULET*

Department of Civil, Geologic and Mining Engineering
POLYTECHNIQUE MONTRÉAL, CANADA

June 22, 2021

Abstract

Reinforcement learning (RL) has gained increasing interest since the demonstration it was able to reach human performance on video game benchmarks using *deep Q-learning* (DQN). The current consensus for training neural networks on such complex environments is to rely on gradient-based optimization. Although alternative Bayesian deep learning methods exist, most of them still rely on gradient-based optimization, and they typically do not scale on benchmarks such as the Atari game environment. Moreover none of these approaches allow performing the analytical inference for the weights and biases defining the neural network. In this paper, we present how we can adapt the temporal difference Q-learning framework to make it compatible with the *tractable approximate Gaussian inference* (TAGI), which allows learning the parameters of a neural network using a closed-form analytical method. Throughout the experiments with on- and off-policy reinforcement learning approaches, we demonstrate that TAGI can reach a performance comparable to backpropagation-trained networks while using fewer hyperparameters, and without relying on gradient-based optimization.

1 Introduction

Reinforcement learning (RL) has gained increasing interest since the demonstration it was able to reach human performance on video game benchmarks using *deep Q-learning* (DQN) [17, 26]. Deep RL methods typically require an explicit definition of an exploration-exploitation function in order to compromise between using the current policy and exploring the potential of new

*Correspondence: luong-ha.nguyen@polymtl.ca, james.goulet@polymtl.ca

actions. Such an issue can be mitigated by opting for a Bayesian approach where the selection of the optimal action to follow is based on Thompson sampling [23]. Bayesian deep learning methods based on variational inference [12, 10, 5, 14, 20, 29], Monte-Carlo dropout [8], or Hamiltonian Monte-Carlo sampling [18] have shown to perform well on regression and classification benchmarks, despite being generally computationally more demanding than their deterministic counterparts. Note that none of these approaches allow performing the analytical inference for the weights and biases defining the neural network. Goulet et al. [9] recently proposed the *tractable approximate Gaussian inference* (TAGI) method which allows learning the parameters of a neural network using a closed-form analytical method. For convolutional architectures applied on classification benchmarks, this approach was shown to exceed the performance of other Bayesian and deterministic approaches based on gradient backpropagation, and to do so while requiring a smaller number of training epochs [19].

In this paper, we present how can we adapt the temporal difference Q-learning framework [24, 28] to make it compatible with TAGI. Section 2 first reviews the theory behind TAGI and the expected value formulation through the Bellman’s Equation. Then, we present how the action-value function can be learned using TAGI. Section 3 presents the related work associated with Bayesian reinforcement learning, and Section 4 compares the performance of a simple TAGI-DQN architecture with the one obtained for its backpropagation-trained counterpart.

2 TAGI-DQN Formulation

This section presents how to adapt the DQN frameworks in order to make them compatible with analytical inference. First, Section 2.1 reviews the fundamental theory behind TAGI, and Section 2.1 reviews the concept of long-term expected value through the Bellman’s equation [25]. Then, Section 2.3 presents how to make the Q-learning formulation [28] compatible with TAGI.

2.1 Tractable Approximate Gaussian Inference

TAGI [9] relies on two main steps; *forward uncertainty propagation* and *backward update*. The first forward uncertainty propagation step is intended to build the joint prior between the neural network parameters and the hidden states. This operation is made by propagating the uncertainty from the model parameters and the input layer through the neural network. TAGI

relies on the Gaussian assumption for the prior of parameters as well as for the variables in the input layer. In order to maintain the analytical tractability of the forward step, we rely on the *Gaussian multiplicative approximation* (GMA) which consists in approximating the product of two Gaussians by a Gaussian random variable whose moments match those calculated exactly using moment generating functions. In order to propagate uncertainty through non-linear activation functions, a second approximation made by locally linearizing these function at the expected value of the hidden unit being activated. Although this linearization procedure may seem to be a crude approximation, it has been shown to match or exceeds the state-of-the-art performance on fully-connected neural networks (FNN) [9], as well as convolutional neural networks (CNN) and generative adversarial networks [19]. TAGI succeeds in maintaining a linear computational complexity for the forward steps, (1) by assuming a diagonal covariance for all parameters in the network and for all the hidden units within a same layer, and (2) by adopting a layer-wise approach where the joint prior is only computed and stored for the hidden units on pairs of successive hidden layers, as well as the hidden units within a layer and the parameters connecting into it. This layer-wise approach is allowed by the inherent conditional independence that is built-in feed-forward neural network architectures.

The second backward update-step consists in performing layer-wise recursive Bayesian inference which goes from hidden-layer to hidden-layer and from hidden-layer to the parameters connecting into it. Given the Gaussian approximation for the joint prior throughout the network, the inference can be done analytically while still maintaining a linear computational complexity with respect to the number of weight parameters in the network. TAGI allows inferring the diagonal posterior knowledge for weights and bias parameters, either using one observation at a time, or using mini-batches of data. As we will show in the next sections, this online learning capacity is best suited for RL problems where we experience episodes sequentially and where we need to define a tradeoff between exploration and exploitation, as a function of our knowledge of the expected value associated with being in a state and taking an action.

2.2 Expected Value and Bellman’s Equation

We define $r(\mathbf{s}, a, \mathbf{s}')$ as the reward for being in a state $\mathbf{s} \in \mathbb{R}^S$, taking an action $a \in \mathcal{A} = \{a_1, a_2, \dots, a_A\}$, and ending in a state $\mathbf{s}' \in \mathbb{R}^S$. For simplicity, we use the short-form notation for the reward $r(\mathbf{s}, a, \mathbf{s}') \equiv r(\mathbf{s})$ in order to

define the value as the infinite sum of discounted rewards

$$v(\mathbf{s}) = \sum_{k=0}^{\infty} \gamma^k r(\mathbf{s}_{t+k}). \quad (1)$$

As we do not know what will be the future states \mathbf{s}_{t+k} for $k > 0$, we need to consider them as random variables (\mathbf{S}_{t+k}), so that the value $V(\mathbf{s}_t)$ becomes a random variable as well,

$$V(\mathbf{s}_t) = r(\mathbf{s}_t) + \sum_{k=1}^{\infty} \gamma^k r(\mathbf{S}_{t+k}). \quad (2)$$

Rational decisions regarding which action to take among the set \mathcal{A} is based the maximization of the expected value as defined by the *action-value* function

$$q(\mathbf{s}_t, a_t) = \mu_V \equiv \mathbb{E}[V(\mathbf{s}_t, a_t, \pi)] = r(\mathbf{s}_t) + \mathbb{E} \left[\sum_{k=1}^{\infty} \gamma^k r(\mathbf{S}_{t+k}) \right], \quad (3)$$

where it is assumed that at each time t , the agent takes the action defined in the policy π . In the case of episode-based learning where the agent interacts with the environment, we assume we know the tuple of states \mathbf{s}_t and \mathbf{s}_{t+1} , so that we can redefine the value as

$$\begin{aligned} V(\mathbf{s}_t, a_t) &= r(\mathbf{s}_t) + \gamma \left(r(\mathbf{s}_{t+1}) + \sum_{k=1}^{\infty} \gamma^k r(\mathbf{S}_{t+1+k}) \right) \\ &= r(\mathbf{s}_t) + \gamma V(\mathbf{s}_{t+1}, a_{t+1}). \end{aligned} \quad (4)$$

Assuming that the value $V \sim \mathcal{N}(v; \mu_V, \sigma_V^2)$ in Equations 2 and 4 is described by Gaussian random variables, we can reparameterize these equations as the sum of the expected value $q(\mathbf{s}, a)$ and a zero-mean Gaussian random variable $\mathcal{E} \sim \mathcal{N}(\epsilon; 0, 1)$, so that

$$V(\mathbf{s}, a) = q(\mathbf{s}, a) + \sigma_V \mathcal{E}, \quad (5)$$

where the variance σ_V^2 and \mathcal{E} are assumed here to be independent of \mathbf{s} and a . Although in a more general framework this assumption could be relaxed, such an heteroscedastic variance term is outside from the scope of this paper. Using this reparameterization, we can write Equation 4 as the discounted difference between the expected values of two subsequent states

$$\begin{aligned} q(\mathbf{s}_t, a_t) &= r(\mathbf{s}_t) + \gamma q(\mathbf{s}_{t+1}, a_{t+1}) - \sigma_{V_t} \mathcal{E}_t + \gamma \sigma_{V_{t+1}} \mathcal{E}_{t+1} \\ &= r(\mathbf{s}_t) + \gamma q(\mathbf{s}_{t+1}, a_{t+1}) + \sigma_V \mathcal{E}. \end{aligned} \quad (6)$$

Note that in Equation 6, σ_{V_t} and $\gamma\sigma_{V_{t+1}}$ can be combined in a single standard deviation parameters σ_V with the assumption that $\mathcal{E}_i \perp \mathcal{E}_j, \forall i \neq j$.

In the case where at a time t , we want to update the Q-values encoded in the neural net only after observing n -step returns [15], we can reformulate the observation equation so that

$$q(\mathbf{s}_t, a_t) = \sum_{i=0}^{n-t-1} \gamma^i r(\mathbf{s}_{t+i}) + \gamma^{n-t} q(\mathbf{s}_n, a_n) + \sigma_V \mathcal{E}_t, \forall t = \{1, 2, \dots, n-1\}. \quad (7)$$

Note that in the application of Equation 7, we employ the simplifying assumption that $\mathcal{E}_t \perp \mathcal{E}_{t+i}, \forall i \neq 0$, as Equation 6 already makes simplifying assumptions for the independence of σ_V^2 and \mathcal{E} . Note that in a more general framework, this assumption could be relaxed. An example of n -step returns is presented in the the algorithm displayed in §1 from the supplementary material.

The following subsections will present, for the case of categorical actions, how to model the deterministic action-value function $q(\mathbf{s}, a)$ using a neural network.

2.3 TAGI Deep Q-learning for Categorical Actions

Suppose we represent the environment’s state at a time t and $t + 1$ by $\{\mathbf{s}, \mathbf{s}'\}$, and the expected value for each of the A possible actions $a \in \mathcal{A}$ by the vector $\mathbf{q} \in \mathbb{R}^A$. In that context, the role of the neural network is to model the relationships between $\{\mathbf{s}, a\}$ and \mathbf{q} . Figure 1a presents a directed acyclic graph (DAG) describing the interconnectivity in such a neural network, where red nodes denote state variables, green nodes are vectors of hidden units \mathbf{z} , the blue box is a compact representation for the structure of a convolutional neural network, and where gray arrows represent the weights and bias $\boldsymbol{\theta}$ connecting the different hidden layers. Note that unlike other gray arrows, the red ones in (b) are not directed arcs representing dependencies, but they simply outline the flow of information that takes place during the inference step. For simplification purposes, the convolutional operations are omitted and all regrouped under the CNN box [19]. In order to learn the parameters $\boldsymbol{\theta}$ of such a network, we need to expand the graph from Figure 1a to include the reward r , the error term $\sigma_V \epsilon$, and \mathbf{q}' , the q -values of the time step $t + 1$. This configuration is presented in Figure 1b where the nodes that have been doubled represent the states \mathbf{s} and \mathbf{s}' which are both evaluated in a network sharing the same parameters. When applying Equation 6, q -values corresponding to a specific action can be selected using

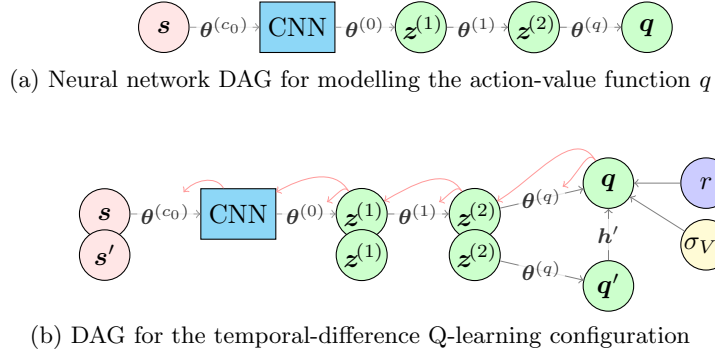


Figure 1: Graphical representation of a neural network structure for temporal-difference Q-learning with categorical actions. The red nodes denote state variables, green nodes are vectors of hidden units \mathbf{z} , and the blue box is a compact representation for the structure of a convolutional neural network. The gray arrows represent the weights and bias $\boldsymbol{\theta}$ connecting the different hidden layers and the red arrows outline the flow of information that takes place during the inference step.

a vector $\mathbf{h}_i \in \{0, 1\}^A$ having a single non-zero value for the i -th component identifying which action was taken at a time t so that

$$q_i = [\mathbf{q}]_i = \mathbf{h}_i^\top \mathbf{q}. \quad (8)$$

During the network’s training, analogously to Thompson sampling [23], the vector $\mathbf{h}'_i \in \{0, 1\}^A$ is defined such that the i -th non-zero value corresponds to the index of the largest value among \mathbf{q}' , a vector of realizations from the neural network’s posterior predictive output $\mathbf{Q} \sim \mathcal{N}(\mathbf{q}'; \boldsymbol{\mu}_{\mathbf{Q}|\mathcal{D}}, \boldsymbol{\Sigma}_{\mathbf{Q}|\mathcal{D}})$. Because of the Gaussian assumptions in TAGI, this posterior predictive is readily available from the forward uncertainty propagation step, as outlined in §2.1.

The red arrows in Figure 1b outline the flow of information during the inference procedure. The first step consists in inferring \mathbf{q} using the relationships defined in either Equation 6 or 7. As this is a linear equation involving Gaussian random variables, the inference is analytically tractable. From there, one can follow the same layer-wise recursive procedure proposed by Goulet et al. [9] in order to learn the weights and biases in $\boldsymbol{\theta}$. With the exclusion of the standard hyperparameters related to network architecture, batch size, buffer size or the discount factor, this TAGI-DQN framework only involves a single hyperparameter, σ_V , the standard deviation for the value function. Note that when using CNNs with TAGI, Nguyen and Goulet

[19] recommended using a decay function for the standard deviation of the observation noise so that at after seing e batches of n -steps,

$$\sigma_V^e = \max(\sigma_V^{\min}, \eta \cdot \sigma_V)^{e-1}. \quad (9)$$

The model in Equation 9 has three hyperparameters, the minimal noise parameter σ_V^{\min} , the decay factor η and the initial noise parameter σ_V . As it was shown by Nguyen and Goulet [19] for CNNs and how we show in §4 for RL problems, TAGI’s performance is robust towards the selection of these hyperparameters.

A comparison of implementation between TAGI and backpropagation on deep Q-network with experience replay [17] is shown in Figure 2. A practical implementation of n -step TAGI deep Q-learning is presented in Algorithm 1 from the supplementary material.

Algorithm 1: TAGI-DQN with Experience Replay	Algorithm 2: DQN with Experience Replay
<pre> 1 Initialize replay memory \mathcal{R} to capacity N; Σ_V; 2 Initialize parameters θ; 3 Discount factor γ; 4 for $episode = 1 : E$ do 5 Reset environment s_0; 6 for $t = 1 : T$ do 7 $q(s_t, a) : Q(s_t, a) \sim \mathcal{N}(\mu_\theta^Q(s_t, a), \Sigma_\theta^Q(s_t, a))$; 8 $a_t = \arg \max_{a \in \mathcal{A}} q(s_t, a)$; 9 $s_{t+1}, r_t = \text{enviroment}(a_t)$; 10 Store $\{s_t, a_t, r_t, s_{t+1}\}$ in \mathcal{R}; 11 Sample random batch of $\{s_j, a_j, r_j, s_{j+1}\}$; 12 $q(s_{j+1}, a') : Q(s_{j+1}, a') \sim \mathcal{N}(\mu_\theta^Q(s_{j+1}, a'), \Sigma_\theta^Q(s_{j+1}, a'))$; 13 $a'_{j+1} = \arg \max_{a' \in \mathcal{A}} q(s_{j+1}, a')$; 14 $\mu_j^y = r_j + \gamma \mu_\theta^Q(s_{j+1}, a'_{j+1})$; 15 $\Sigma_j^y = \gamma^2 \Sigma_\theta^Q(s_{j+1}, a'_{j+1}) + \Sigma_V$; 16 Update θ using TAGI on PDF(θy) </pre>	<pre> 1 Initialize replay memory \mathcal{R} to capacity N ; 2 Initialize parameters θ; 3 Discount factor γ; 4 Define ϵ (epsilon-greedy function); 5 for $episode = 1 : E$ do 6 Reset environment s_0; 7 for $t = 1 : T$ do 8 $u : U \sim \mathcal{U}(0, 1)$; 9 $a_t = \begin{cases} \text{randi}(A) & u < \epsilon; \\ \arg \max_{a \in \mathcal{A}} Q_\theta(s_t, a) & u \geq \epsilon; \end{cases}$ 10 $s_{t+1}, r_t = \text{enviroment}(a_t)$; 11 Store $\{s_t, a_t, r_t, s_{t+1}\}$ in \mathcal{R}; 12 Sample random batch of $\{s_j, a_j, r_j, s_{j+1}\}$; 13 $y_j = r_j + \gamma \max_{a' \in \mathcal{A}} Q_\theta(s_{j+1}, a')$; 14 Update θ using gradient descent on 15 $L = 0.5 [y_j - Q_\theta(s_j, a_j)]^2$; </pre>

Figure 2: Comparison of TAGI with backpropagation on deep Q-network with experience replay. PDF: probability density function; L : loss function; \mathcal{U} : uniform distribution; **randi**: uniformly distributed pseudorandom integers.

3 Related Work

Over the last decades, several approximate methods have been proposed in order to allow for Bayesian neural networks [18, 12, 10, 5, 14, 20, 29, 8] with

various degree of approximations. Although some these methods have shown to be capable of tackling classification tasks on datasets such ImageNet [20], few of them have been applied on large-scale RL benchmark problems. The key idea behind using Bayesian methods for reinforcement learning is to consider the uncertainty associated with Q-functions in order to identify a tradeoff between exploring the performance of possible actions and exploiting the current optimal policy [25]. This typically takes the form of performing Thompson sampling [23] rather than relying on heuristics such as ϵ -greedy.

For instance, MC dropout [8] was introduced has a method intrinsically suited for reinforcement learning. Nevertheless, five years after its inception, the approach has not yet been reliably scaled to more advanced benchmarks such as the Atari game environment. The same applies to Bayes-by-backprop [5] which was recently applied to simple RL problems [13], and which has not yet been applied to more challenging environments requiring convolutional networks. On the other hand, Bayesian neural networks relying on sampling methods such as Hamiltonian Monte-Carlo [18] are typically computationally demanding to be scaled to RL problems involving such a complex environment.

Although mainstream methods related to Bayesian neural networks have seldom been applied to complex RL problems, several research teams have worked on alternative approaches in order to allow performing Thompson sampling. For instance, Azizzadenesheli et al. [4] have employed a deep Q-network where the output layer relies on Bayesian linear regression. This approach was shown to be outperforming its deterministic counterparts on Atari games. Another approach by Osband et al. [21] employs bootstrapped deep Q-networks with multiple network heads in order to represent the uncertainty in the Q-functions. This approach was also shown to scale to Atari games while presenting an improved performance in comparison with deterministic deep Q-networks. Finally, Wang and Zhou [27] have tackled the same problem, but this time by modelling the variability in the Q-functions through a latent space learned using variational inference. Despite its good performance on the benchmarks tested, it did not allowed to be scaled to the Atari game environment.

The TAGI deep Q-network presented in th is paper is the first demonstration that an analytically tractable inference approach for Bayesian neural networks can be scaled to a problem as challenging as the Atari game environment.

4 Benchmarks

This section compares the performance of TAGI with backpropagation-based standard implementations on off- and on-policy deep RL. For the off-policy RL, both TAGI-based and backpropagation-based RL approaches are applied to deep Q-learning with experience replay (see Algorithm 1 & 2) for the lunar lander and cart pole environments. For the on-policy RL, TAGI is applied to the n -step Q-learning algorithm and is compared with its backpropagation-based counterpart [15]. We perform the comparison for five Atari games including Beamrider, Breakout, Pong, Qbert, and Space Invaders. Note that these five games are commonly selected for tuning hyperparameters for the entire Atari games [15, 16]. All benchmark environments are taken from the OpenAI Gym [6].

4.1 Experimental Setup

In the first experiments with off-policy RL, we use a fully-connected multi-layer perceptron (MLP) with two hidden layers of 256 units for the lunar lander environment, and with one hidden layer of 64 units for the cart pole environment. In these experiments, there is no need for input processing nor for reward normalization. Note that unlike for the deterministic Q-network, TAGI does not use a target Q-network for ensuring the stability during training and allows eliminating the hyperparameter related to the target update frequency. For the deep Q-network trained with backpropagation, we employ the pre-tuned implementation of OpenAI baselines [7] with all hyperparameters set to the default values.

For the Atari experiments with on-policy RL, we use the same input processing and model architecture as Mnih et al. [15]. The Q-network uses two convolutional layers (16-32) and a full-connected MLP of 256 units. TAGI n -step Q-learning only uses a single network to represent the value function for each action, and relies on a single learning agent. The reason behind this choice is that TAGI current main library is only available on Matlab which does not support running a Python multiprocessing module such as the OpenAI gym. In the context of TAGI, we use an horizon of 128 steps and as recommended by Andrychowicz et al. [3] and following practical implementation details [1, 2], each return in n -step Q-learning algorithm is normalized by subtracting the average return from the current n -steps and then dividing by the empirical standard deviation from the set of n returns. The standard deviation for the value function, (σ_V) , is initialized at 2. σ_V is decayed each 128 steps with a factor $\eta = 0.9999$.

The minimal standard deviation for the value function $\sigma_V^{\min} = 0.3$. These hyperparameters values were not grid-searched but simply adapted to the scale of the problems and are kept constant for all experiments. The complete details of the network architecture and hyperparameters are provided in the supplementary material.

4.2 Results

For the first set of experiments using off-policy RL, Figure 3 presents the average reward over 100 episodes for three runs for the lunar lander and cart pole environment. The TAGI-based deep Q-learning with experience replay shows a faster and more stable learning than the one relying on backpropagation, while not requiring a target network.

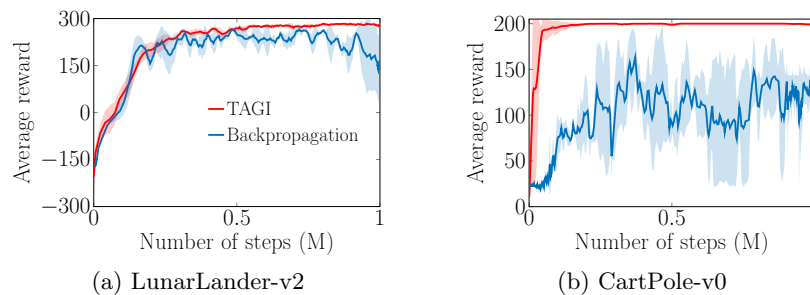


Figure 3: Illustration of average rewards over 100 episodes of three runs for one million time steps for the TAGI-based and backpropagation-based deep Q-learning.

Table 1 shows that the average reward over the last 100 episodes obtained using TAGI are greater than the one obtained using backpropagation.

Table 1: Average reward over the last 100 episodes for the lunar lander and cart pole experiments. TAGI: Tractable Approximate Gaussian Inference.

Method	Lunar lander	Cart pole
TAGI	277.6 ± 6.3	199.2 ± 1.3
Backpropagation	166.7 ± 103.6	130.3 ± 16.9

Figure 4 compares the average reward over 100 episodes for three runs obtained for TAGI, with the results from Mnih et al. [15] for the second set of experiments on Atari games. Note that all results presented were obtained for a single agent, and that the results for the backpropagation-trained networks are only reported at the end of each epoch.

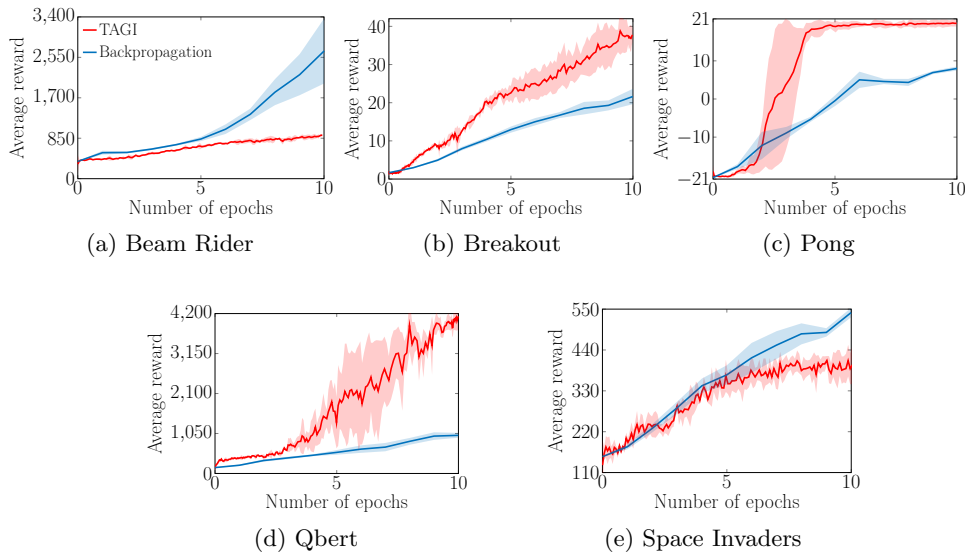


Figure 4: Illustration of average reward over 100 episodes of three runs for five Atari games. The number of epochs is used here for the comparison of TAGI and backpropagation-trained counterpart obtained by Mnih et al. [15]. Each epoch corresponds to four million frames. The environment identity are $\{Atari\ Game\}NoFrameSkip-v4$.

Results show that TAGI outperforms the results from the original n -step Q-learning algorithm trained with backpropagation [15] on Breakout, Pong, and Qbert, while underperforming on Beam Rider and Space Invaders. The average training time of TAGI for an Atari game is approximately 13 hours on GPU calculations benchmarked on a 4-core-intel desktop of 32 GB of RAM with a NVIDIA GTX 1080 Ti GPU. The training speed of TAGI for the experiment of the off-policy deep RL is approximately three times slower on CPU calculations than the backpropagation-trained counterpart. The reason behind this slower training time is because of its intrinsically different inference engine, so that TAGI’s implementation is not compatible with existing libraries such as TensorFlow or Pytorch. TAGI’s

library development is still ongoing and it is not yet fully optimized for computational efficiency. Overall, these results for on- and off policy RL approaches confirm that TAGI can be applied to large scale problems such as deep Q-learning.

5 Discussion

Although the performance of TAGI does not systematically outperform its backpropagation-based counterpart, it requires fewer hyperparameters (see §3 in supplementary material). This advantage is one of the key aspects for improving the generalization and reducing the computational cost of the hyperparameter tuning process which are the key challenges in current state of deep RL [11]. For instance, in this paper, the TAGI’s hyperparameters relating to the standard deviation of value function (σ_V) are kept constant across all experiments. Moreover, since these hyperparameters were not subject to grid-search in order to optimize the performance, the results obtained here are representative of what a user should obtain by simply adapting the hyperparameters to fit the specificities and scale of the environment at hand.

More advanced RL approaches such as advanced actor critic (A2C) [15] and proximal policy optimization (PPO) [22] employ two-networks architectures in which one network is used to approximate a value function and other is employed to encode the policy. The current TAGI-RL framework is not yet able to handle such architectures because training a policy network involves an optimization problem for the selection of the optimal action. Backpropagation-based approach currently rely on gradient optimization to perform this task, while TAGI will require developing alternative approaches in order to maintain the analytical tractability without relying on gradient-based optimization.

6 Conclusion

This paper presents how to adapt TAGI to deep Q-learning; Throughout the experiments, we demonstrated that TAGI could reach a performance comparable to backpropagation-trained networks while using fewer hyperparameters. These results challenge the common belief that for large scale problems such as the Atari environment, neural networks can only be trained by relying on gradient backpropagation. We have shown here that this current paradigm is no longer the only alternative as TAGI has a linear computational complexity

and can be used to learn the parameters complex networks in an analytically tractable manner, without relying on gradient-based optimization.

Acknowledgements

The first author was financially supported by research grants from Hydro-Quebec, and the Natural Sciences and Engineering Research Council of Canada (NSERC).

References

- [1] Pytorch examples for reinforce algorithm. https://github.com/pytorch/examples/blob/master/reinforcement_learning/reinforce.py, 2019.
- [2] Pytorch examples for actor critic algorithm. https://github.com/pytorch/examples/blob/master/reinforcement_learning/actor_critic.py, 2020.
- [3] M. Andrychowicz, A. Raichuk, P. Stańczyk, M. Orsini, S. Girgin, R. Marinier, L. Hussenot, M. Geist, O. Pietquin, M. Michalski, S. Gelly, and O. Bachem. What matters for on-policy deep actor-critic methods? a large-scale study. In *International Conference on Learning Representations*, 2021.
- [4] K. Azizzadenesheli, E. Brunskill, and A. Anandkumar. Efficient exploration through Bayesian deep q-networks. In *IEEE Information Theory and Applications Workshop*, pages 1–9, 2018.
- [5] C. Blundell, J. Cornebise, K. Kavukcuoglu, and D. Wierstra. Weight uncertainty in neural networks. *arXiv preprint arXiv:1505.05424*, 2015.
- [6] G. Brockman, V. Cheung, L. Pettersson, J. Schneider, J. Schulman, J. Tang, and W. Zaremba. Openai gym. *arXiv preprint arXiv:1606.01540*, 2016.
- [7] P. Dhariwal, C. Hesse, O. Klimov, A. Nichol, M. Plappert, A. Radford, J. Schulman, S. Sidor, Y. Wu, and P. Zhokhov. Openai baselines. <https://github.com/openai/baselines>, 2017.
- [8] Y. Gal and Z. Ghahramani. Dropout as a bayesian approximation: Representing model uncertainty in deep learning. In *ICML proceedings*, pages 1050–1059, 2016.
- [9] J-A. Goulet, L.H. Nguyen, and S. Amiri. Tractable approximate Gaussian inference for Bayesian neural networks. *arXiv preprint*, 2020.
- [10] J. M. Hernández-Lobato and R. Adams. Probabilistic backpropagation for scalable learning of bayesian neural networks. In *International Conference on Machine Learning*, pages 1861–1869, 2015.
- [11] A. Irpan. Deep reinforcement learning doesn't work yet. <https://www.alexirpan.com/2018/02/14/rl-hard.html>, 2018.

- [12] D. P. Kingma, T. Salimans, and M. Welling. Variational dropout and the local reparameterization trick. In C. Cortes, N. Lawrence, D. Lee, M. Sugiyama, and R. Garnett, editors, *Advances in Neural Information Processing Systems*, volume 28, 2015.
- [13] Z. Lipton, X. Li, J. Gao, L. Li, F. Ahmed, and L. Deng. Bbq-networks: Efficient exploration in deep reinforcement learning for task-oriented dialogue systems. In *Proceedings of the AAAI Conference on Artificial Intelligence*, volume 32, 2018.
- [14] C. Louizos and M. Welling. Structured and efficient variational deep learning with matrix Gaussian posteriors. In *ICML proceedings*, pages 1708–1716, 2016.
- [15] V. Mnih, Adria P. Badia, M. Mirza, A. Graves, T. Lillicrap, T. Harley, D. Silver, and K. Kavukcuoglu. Asynchronous methods for deep reinforcement learning. In *ICML proceedings*, pages 1928–1937. PMLR, 2016.
- [16] V. Mnih, K. Kavukcuoglu, D. Silver, A. Graves, I. Antonoglou, D. Wierstra, and M. Riedmiller. Playing atari with deep reinforcement learning. *arXiv preprint arXiv:1312.5602*, December 2013.
- [17] V. Mnih, K. Kavukcuoglu, D. Silver, A.A. Rusu, J. Veness, M.G. Bellemare, A. Graves, M. Riedmiller, A.K. Fidjeland, and G Ostrovski. Human-level control through deep reinforcement learning. *nature*, 518(7540):529–533, 2015.
- [18] R. M. Neal. *Bayesian learning for neural networks*. PhD thesis, University of Toronto, 1995.
- [19] L. H. Nguyen and J-A. Goulet. Analytically tractable inference in deep neural networks. *arXiv preprint*, 2021.
- [20] K. Osawa, S. Swaroop, A. Jain, R. Eschenhagen, R. E. Turner, R. Yokota, and M. E. Khan. Practical deep learning with Bayesian principles. In *Advances in Neural Information Processing Systems proceedings*, 2019.
- [21] I. Osband, C. Blundell, A. Pritzel, and Benjamin V. Roy. Deep exploration via bootstrapped dqn. In *NEURIPS proceedings*, pages 4033–4041, 2016.
- [22] J. Schulman, F. Wolski, P. Dhariwal, A. Radford, and O. Klimov. Proximal policy optimization algorithms. *arXiv preprint arXiv:1707.06347*, 2017.
- [23] M. Strens. A Bayesian framework for reinforcement learning. In *ICML proceedings*, pages 943–950, 2000.
- [24] R. S. Sutton. Learning to predict by the methods of temporal differences. *Machine learning*, 3(1):9–44, 1988.
- [25] R. S. Sutton and A. G. Barto. *Reinforcement learning: An introduction*. MIT Press, 2nd edition, 2018.
- [26] H. Van Hasselt, A. Guez, and D. Silver. Deep reinforcement learning with double q-learning. In *Proceedings of the AAAI Conference on Artificial Intelligence*, volume 30, 2016.

- [27] Z. Wang and M. Zhou. Thompson sampling via local uncertainty. In *ICML proceedings*, volume 119, pages 10115–10125, 13–18 Jul 2020.
- [28] C. J. Watkins and P. Dayan. Q-learning. *Machine learning*, 8(3-4):279–292, 1992.
- [29] A. Wu, S. Nowozin, E. Meeds, R. E. Turner, J. M. Hernández-Lobato, and A. L. Gaunt. Deterministic variational inference for robust Bayesian neural networks. In *ICLR proceedings*, 2019.

A Algorithm

This section presents the n -steps Q-learning algorithm with Tractable Approximate Gaussian Inference (TAGI).

Algorithm 3: n -step Q-learning with TAGI

```

1 Initialize  $\theta$  ;  $\Sigma_V$ ; number of steps ( $N$ )
2 Initialize memory  $\mathcal{R}$  to capacity  $N$ ;
3 steps = 0;
4 for episode = 1 : E do
5   Reset environment  $s_0$ ;
6   for  $t = 1 : T$  do
7     steps = steps + 1;
8      $q(s_t, a) : Q(s_t, a) \sim \mathcal{N}(\mu_{\theta}^Q(s_t, a), \Sigma_{\theta}^Q(s_t, a))$ ;
9      $a_t = \arg \max_{a \in \mathcal{A}} q(s_t, a)$ ;
10     $s_{t+1}, r_t = \text{enviroment}(a_t)$ ;
11    Store  $\{s_t, a_t, r_r\}$  in  $\mathcal{R}$ ;
12    if steps mod N == 0 then
13       $q(s_{t+1}, a') : Q(s_{t+1}, a') \sim \mathcal{N}(\mu_{\theta}^Q(s_{t+1}, a'), \Sigma_{\theta}^Q(s_{t+1}, a'))$ ;
14       $a'_{t+1} = \arg \max_{a \in \mathcal{A}} q(s_{t+1}, a')$ ;
15      Take  $N$  samples of  $\{s_j, a_j, r_j\}$  from  $\mathcal{R}$ ;
16       $\mu_N^y = \mu_{\theta}^Q(s_{t+1}, a'_{t+1})$ ;  $\Sigma_N^y = \Sigma_{\theta}^Q(s_{t+1}, a'_{t+1})$ ;
17      for  $j = N - 1 : 1$  do
18         $\mu_j^y = r_j + \gamma \mu_{j+1}^y$ ;  $\Sigma_j^y = \gamma^2 \Sigma_{j+1}^y + \Sigma_V$ ;
19      Update  $\theta$  using TAGI;
20      Initialize memory  $\mathcal{R}$  to capacity  $N$ ;

```

B Model Architecture

This appendix contains the specifications for each model architecture in the experiment section. D refers to a layer depth; W refers to a layer width; H refers to the layer height in case of convolutional or pooling layers; K refers to the kernel size; P refers to the convolutional kernel padding; S refers to the convolution stride; σ refers to the activation function type; ReLU refers to rectified linear unit; N_a refers to the number of actions.

Table 2: Model Architecture for Cart pole

Layer	$D \times W \times H$	$K \times K$	P	S	σ
Input	$4 \times 1 \times 1$	-	-	-	-
Full connected	$64 \times 1 \times 1$	-	-	-	ReLU
Output	$2 \times 1 \times 1$	-	-	-	-

Table 3: Model Architecture for Lunar lander

Layer	$D \times W \times H$	$K \times K$	P	S	σ
Input	$8 \times 1 \times 1$	-	-	-	-
Full connected	$256 \times 1 \times 1$	-	-	-	ReLU
Full connected	$256 \times 1 \times 1$	-	-	-	ReLU
Output	$4 \times 1 \times 1$	-	-	-	-

Table 4: Model Architecture for Atari domain

Layer	$D \times W \times H$	$K \times K$	P	S	σ
Input	$4 \times 84 \times 84$	-	-	-	-
Convolutional	$16 \times 20 \times 20$	8×8	0	4	ReLU
Convolutional	$32 \times 9 \times 9$	4×4	0	2	ReLU
Full connected	$256 \times 1 \times 1$	-	-	-	ReLU
Output	$N_a \times 1 \times 1$	-	-	-	-

C Hyperparameter

This appendix details the hyperparameters for each model architecture in the experiment section

Table 5: Hyperparameters for Cart pole and Lunar lander

Method	#	Hyperparameter	Value
TAGI	1	Initial standard deviation for the value function (σ_V)	2
	2	Decay factor (η)	0.9999
	3	Minimal standard deviation for the value function (σ_V^{\min})	0.3
	4	Buffer size	50 000
	5	Batch size	10
	6	Discount (γ)	0.99
Backprop	1	Learning rate	5×10^{-4}
	2	Adam epsilon	10^{-5}
	3	Adam β_1	0.9
	4	Adam β_2	0.999
	5	Buffer size	50 000
	6	Exploration fraction	0.1
	7	Final value of random action probability	0.02
	8	Batch Size	32
	9	Discount (γ)	0.99
	10	Target update frequency	500
	11	Gradient norm clipping coefficient	10

Table 6: Hyperparameters for Atari domain

Method	#	Hyperparameter	Value
TAGI	1	Horizon	128
	2	Initial standard deviation for the value function (σ_V)	2
	3	Decay factor (η)	0.9999
	4	Minimal standard deviation for the value function (σ_V^{\min})	0.3
	5	Batch size	32
	6	Discount (γ)	0.99
	7	Number of actor-learners	1
Backprop	1	Horizon	5
	2	Initial learning rate	<i>LogUniform</i> ($10^{-4}, 10^{-2}$)
	3	Learning rate schedule	<i>LinearAnneal</i> (1, 0)
	4	RMSProp decay parameter	0.99
	5	Exploration rate 1 (ϵ_1)	0.1
	6	Exploration rate 2 (ϵ_2)	0.01
	7	Exploration rate 3 (ϵ_3)	0.5
	8	Probability of exploration rate 1	0.4
	9	Probability of exploration rate 2	0.3
	10	Probability of exploration rate 3	0.3
	11	Exploration rate schedule (first four million frames)	Anneal from 1 to $\epsilon_1, \epsilon_2, \epsilon_3$
	12	Batch size	5
	13	Discount (γ)	0.99
	14	Number of actor-learners	1